Plus Laser deposition to preparation Co-Ninanoparticles ferrite and hyperthermia application

Marwa H.Sabbar *, T. H. Mubarak and Nada S.Ahmad
Department of Physics, College of Science, University of Diyala, Diyala, Iraq
am6645849@gmail.com

Abstract

Nickel-doped cobalt nanoparticles (NPs) were with the chemical formula $Co_{1-x}Ni_xFe_2O_4$ (was, x = 0.0, 0.2, and 0.4).Manufactured at low temperature (70 Cº) using plsd laser deposition technology. Soduim hydroxideis used as a chelating agentwith a mixture of nickel nitrate and ferric nitrate solutions in a ratio (3: 1) to balance the oxidizing agent ratio. The obtained ferrite NPs were calcined at temperatures (300 °C) for 3 h Air to remove water content and unwanted impurities and get a better single-phase spinel structure. Then the obtained powder is compressed into a disc shape with a diameter of (1 cm) and then we use laser deposition technology to get a ferrite membrane where the structural properties of the calcined ferrite sheets are confirmed by analyzing X ray Diffraction (XRD) technique. XRD analysis shows the structure of a single-phase nanoscale spinel. The crystal size calculated from the FWHM of the strongest peak (311) lies in the range (9.04-15 nm) for $Co_{1-x}Ni_xFe_2O_4$ Ferrite NPs. The images of the spherical-shaped and monolithic FE-SEM NPs show the Particle size morphology in the range (12-15 nm), reflecting the highly crystalline nature of these nanoparticles. Particle size and grain size of $Co_{1-x}Ni_xFe_2O_4$ ferrite NPs calculated using XRD and SEM technologies are compatible with each other in the same range

Keywords: Co-Ni-Fe_2O_4 ferrites;magneticnanocomposite;plsd laser deposition technology; antibacterial activity.

DOI Number: 10.14704/nq.2022.20.3.NQ22343 NeuroQuantology 2022; 20(3):533-542

1.Introduction

Ferrites are ferrimagnetic oxides consisting of ferric oxide and metal oxides. On the basis of crystal structure ferrites are grouped into three classes namely hexagonal ferrite, garnet and spinel ferrite The magnetic properties arise from interactions between metallic ions occupying particular positions relative to the oxygen ions in the crystal structure of the oxide. Ferrites with spinel structure represent the important class of magnetic materials. The combination of magnetic and electrical properties makes ferrite useful in many technological applicationsThe spinel ferrite is having the chemical formula MFe2O4 (where M- is a divalent metal ions such as Co, Ni, Mn etc). and possess two sub-lattice namely tetrahedral A and octahedral B sites[1,2]. As an important member in the family of spinel ferrites cobalt ferrite (CoFe2O4) with inverse spinel structure are promising magnetic materials because of

energy and with repetition rates of 1 to 100 Hz. The target is usually scanned by the laser beamwhile being rotated to ensure uniform ablation from the target surface. [4]Pulsed laser deposition is a physical vapor deposition process, which is performed in a vacuum system. The deposition process is very complex, which includes the features of molecular beam epitaxy and sputter deposition pulsed laser with high energy is focused onto the target material to be deposited on thesubstrate. Each laser pulse only vaporizes or ablates a small amount of the target material, and transfers each ablation into a plasma plume. The ablated target material is ejected from the target surface in a highly forward-directed plume toward the substrate and then deposited on the surfac e of the substrate. [5]

their moderate saturation. magnetization, high electrical properties, high magneto-crystalline anisotropy, good mechanical properties and chemical stability [2]. Ferrites or Ferrimagnetics are oxides, dark grey or black in appearance , possesses the properties of ceramic materials, such as being hard, brittle and chemically inert, can be changing the electromagnetic properties of ferrites by controlling the manner of preparation and type of materials used, amount of material added and sintering temperature [3]. In this paper, (Co-Ni)Ferrite was prepared by laser deposition(pld) method Pulsed laser deposition (PLD) technique has been investigated since late 1980s.This technique has been applied successfully to prepare chemically and structurally complex materials. PLD uses a high-power laser which operates at high

2. Experimental work

2.1 Materials and Methods

Table No. (2.1.1) shows the raw materials and their density.

Table (3-1-1) Chemicals Used

Compounds	Chemicalformula	Mol. Mass (g.mol^-1)
Iron nitrate	$Fe(NO_3)_3.9H_2O$	403.8
Cobaltnitrate	$Co(NO_3)_2.6H_2O$	291.031
nickel nitrate	$Ni(NO_3)_2.6H_2O$	290.79
Sodium hydroxide	NaOH	39.9971

the samples and allowing them to cool slowly naturally to check their dielectric properties.

2.3 Pulsed Laser deposition (PLD) Method

Figure 1 shows the experimental setup for laser deposition of solid metal target by pulsed laser deposition.The pulsed laser deposition experiment was carried out inside a vacuum chamber generally in (10-3 mbar) vacuum conditions. The focused Nd:YAG laser beam at 600 mJ with a frequency second radiation at 1064nm (pulse width 9 ns) repetition frequency (3

2.2 calcifications and granule formation

The ferrite powder obtained by CCD is placed in a ceramic vessel and then roasted at 300°C for 3 hours to remove reaction residues such as water or carbon dioxide particles from combustion, resulting in the necessary ferrite powder. Then 0.5 g of burnt samples and samples with concentration (x = 0.0, , 0. 2, and 0.4) round granules 1 cm in diameter and 3 mm thick. This is achieved by pressing 500 tons for five minutes with a hydraulic press using the dry pressing method, then sintering at 300 °C for 3 hours to thicken

the laser was set to (10 cm), and between the target and the substrate was (1.5cm).

Hz), for 650 laser pulses incident on the target surface makes an angle of 45° with it. The distance between the target and

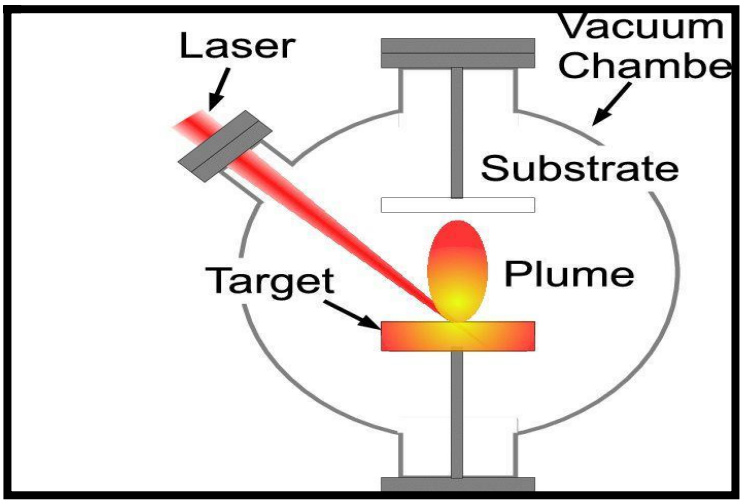

Figure 1: experimental setup for laser deposition

2.4 Antibacterial

cell wall, the shape of the cell membrane, and the ability of the outermost membrane to inhibit the creation of reactive oxygen species (ROS) caused by the metal ions are all taken into consideration. Cell membrane damage, the generation of reactive oxygen species (ROS), DNA damage caused by aerobic respiration, and cell division are all examples of NPs' antimicrobial activity [6-7]

Because of their ability to penetrate cells' walls, Co-Ni-Fe2O4 NCs may cause cells to leak and exocytose, as well as inhibit the activity of essential enzymes. Using the following equation [8, 9]

3. Result and Discussion

3.1 XRD Analyses

The XRD parameters of the $Co_{1-x}Ni_xFe_2O_4$ ferrite nanoparticles calcined at (300°C). Figure (1) show that the crystallite size (D) of the(Co- Ni) ferrites are decreases in the range of (9.04-15.42nm) . Are due to the different ionic radii, Ni+2 (tetrahedral 0.58; octahedral 0.69 Å) and Co+2 (tetrahedral 0.58; octahedral 0.74Å) [10].

activity of Co-Ni-Fe2O4 NCs ferrite nanocomposites

To determine whether or not Co-Ni-Fe2O4 ferrite nanocomposites had the ability to create a zone of inhibition in bacteria in a dose-dependent manner, bacterial cultures were established. In order to demonstrate bactericidal action, the Co-Ni-Fe2O4 NCs ferrite nanocomposites must exhibit a wide zone of inhibition for gram-negative bacteria (E. coli) and a smaller zone of inhibition for gram-positive bacteria (S. aureus). Gram-negative bacteria have a distinct cell wall structure that distinguishes them from their Gram-positive counterparts. Bacterial cells from the Gram-positive group are covered with a thick layer of peptidoglycan that contains lipopolysaccharide as well as phospholipids and proteins [6-7]

This test allows for the clear observation of the bactericidal action of the Co-Ni-Fe2O4 NCs that have been generated in the laboratory. In order to have a bactericidal effect, the thickness of the

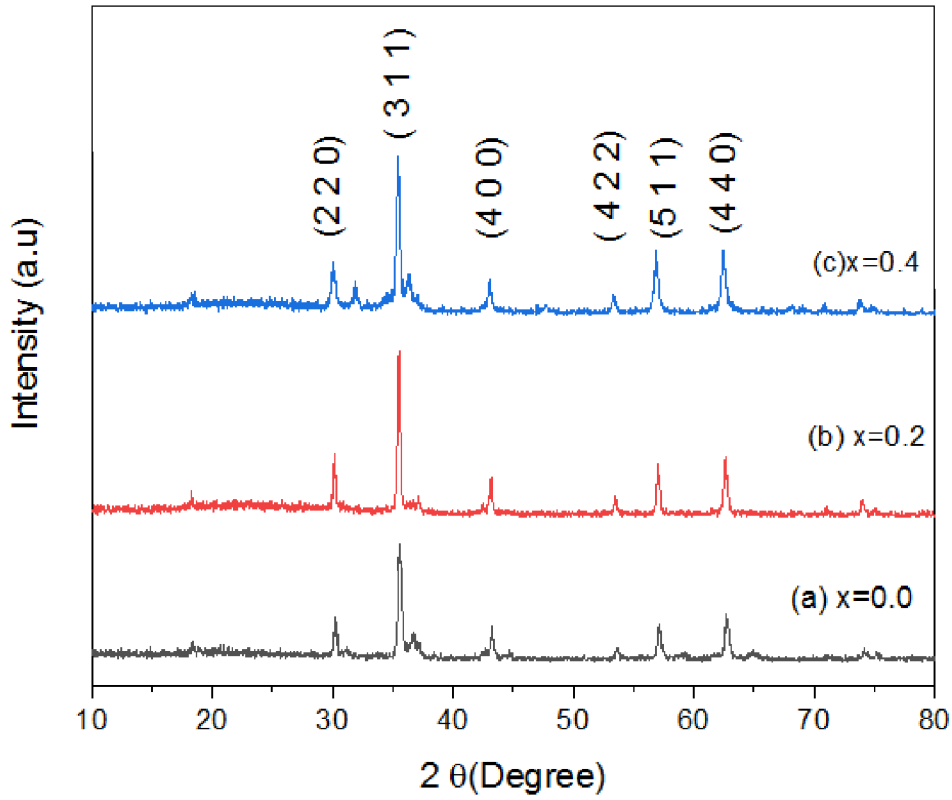

Figure 2 XRD Patterns of synthesized Co_{1-x} Ni_x Fe_2 O_4 Ferrite

Table 2 : XRD parameters of synthesized $Ni_xCo_{1-x}Fe_2O_4$

Material	Ratio	2Θ (deg) Practical	2Θ (deg) Standard	FWHM (deg)	Crystalline size (nm)	D (nm) FE-SEMl	(hkl)
$CoFe_2O_4$	0	35.58	35.42	0.485	15.42	15.470	(113)
$Ni_{0.2}Co_{0.8}Fe_2O_4$	0.2	35.51	35.42	0.784	10.07	12.729	(113)
$Ni_{0.4}Co_{0.6}Fe_2O_4$	0.4	35.70	35.42	0.873	9.04	12.223	(113)

3.2 FTIR Spectroscopy Analysis

Infrared spectrum for spinel ferrites involve two main absorption bands arises due to stretching vibration of both tetrahedral (A-O) and octahedral (BO) sites. Furthermore, it was observed the presence of OH-groups in the spectrum which has been revealed by IR spectrum (bands at 3440 and 1630)[11]. The IR spectrum measurements of samples are given in figure (2). It showed two distinctive absorption bands lie in the region ~564 and ~374 cm^{-1} . The wave number is attributed to stretching vibration of (A-O) site and υ2 is due to stretching vibration of (B-O) site.

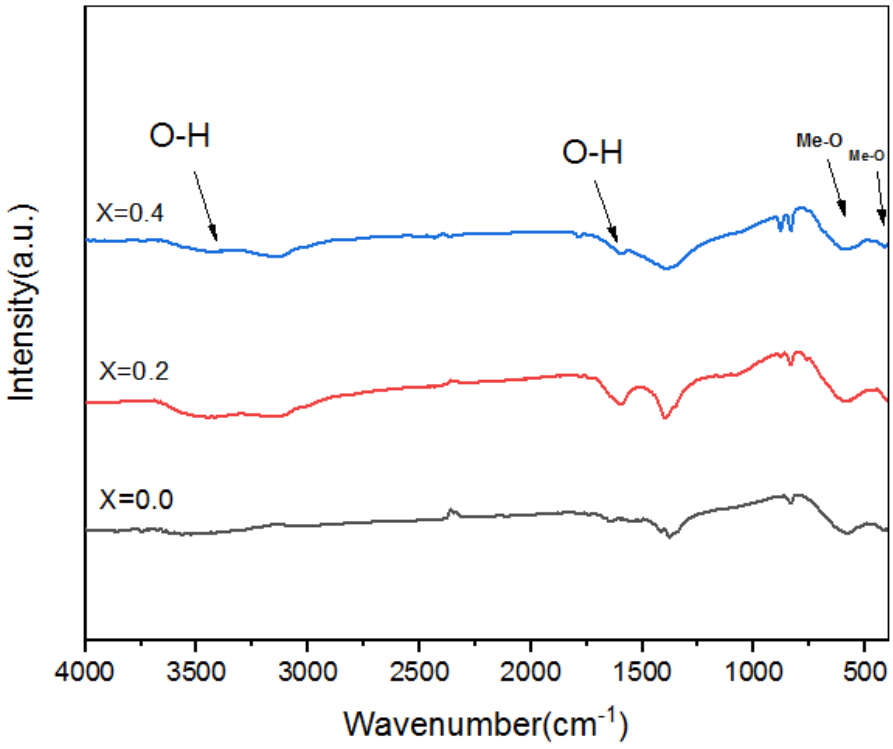

Figur 3:FTIR Spectroscopy Analysis of $Co_{1-x}Ni_xFe_2O_4$

Table 2: IR absorption bands of the samples

X	υ_{Tcm}^{-1}	υ_{Bcm}^{-1}
0.0	574.22	364.81
0.2	567.55	364.48
0.4	566.22	363.48

3.3 FE-SEM Image Analysis

Investigation of nanostructure is vital to comprehend the superparamagnetic properties of polycrystalline ferrites. The particle size and surface morphology of Co_{1-x} Ni_x Fe_2O_4 had been investigated by a set of FE-SEM images as shown in figure (4). All the samples show a spherical shape with narrow size distribution.

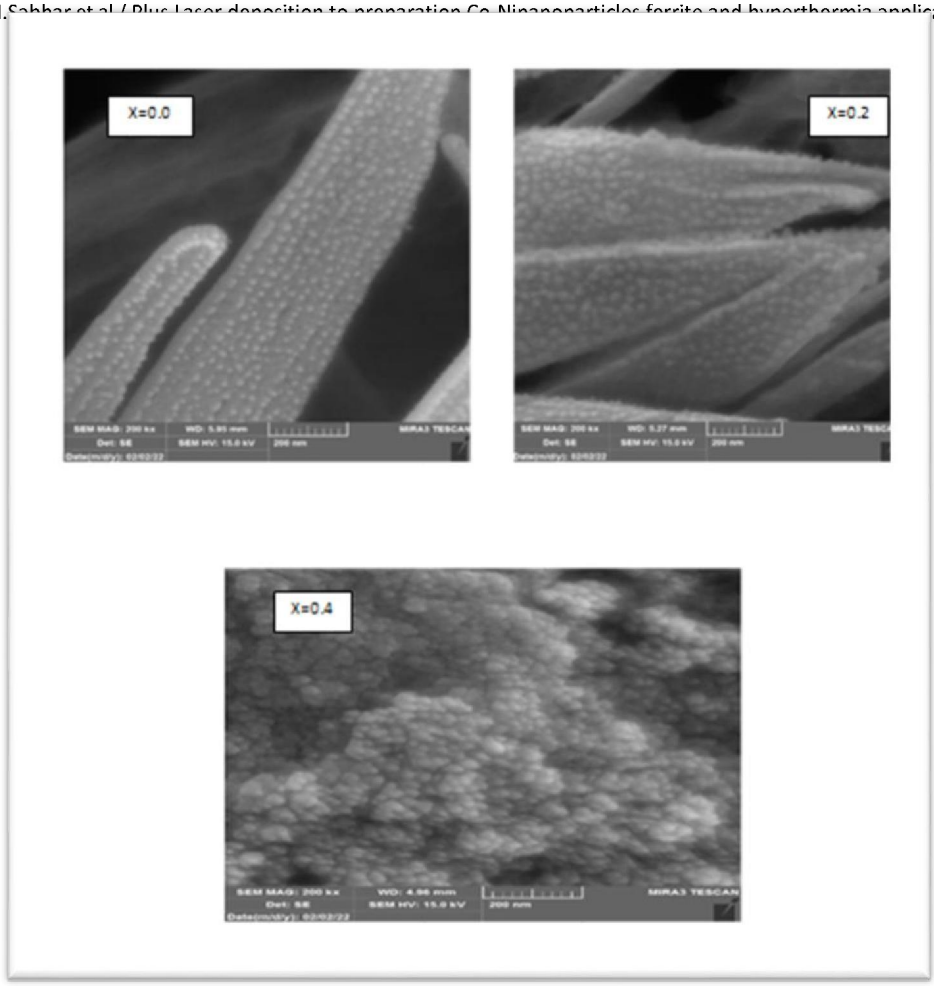

FE-SEM of $Co_{1-X}Ni_XFe_2O_4$ Figur 4:

when x=0.2 but fast decreases with Ni concentration at (x=0.4).

The magnetic order in the cubic spinels is due to the super-exchange interaction mechanism occurring between the metal ions in the tetrahedral A-sites and octahedral B-site sublattices . Substitutional ions (Ni^{2+}) with zero magnetic moment cause the variation in the magnetic properties of the spinel ferrites. The results obtained are in well accordance with the earlier reported values by [12].

3.4 Magnetic Properties

The magnetic properties of the prepared samples are analyzed using a magnetometer (VSM) at room temperature applied field ±15 KOe. Figure. (5)shows the M-H curves of the prepared samples by normal Co-precipitation method .Two prepared samples of Co-Ni ferrite (x = 0.0, 0.2)at room temperature exhibit ferrimagnetic coupling but one of them it superparamagnatic x= (0.4). saturation magnetization and coercivity increasing

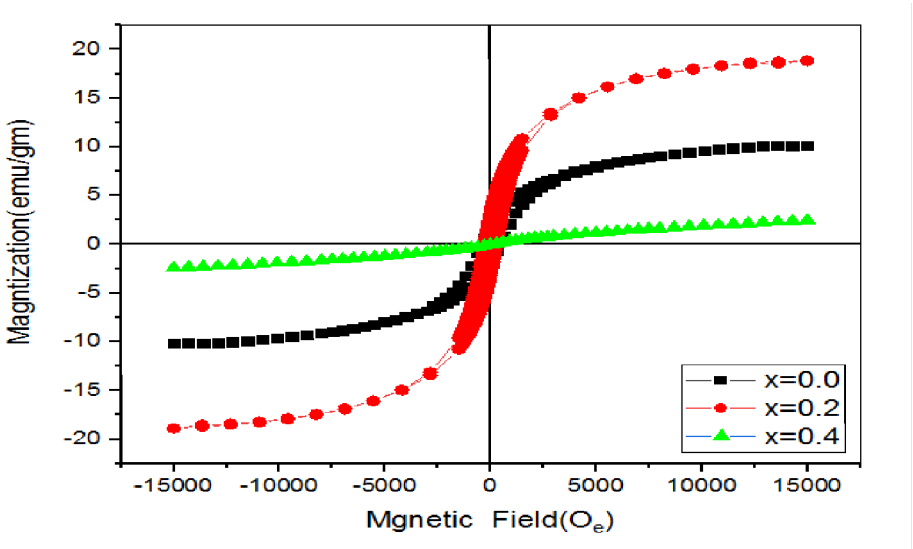

Figure (5): Magnetic hysteresis loops of $Co_{1-x}Ni_xFe_2O_4$ (x=0.0, 0.2, 0.4)

Table(3):The values of saturation magnetization, remanence, coercivity

x	M_S	M_r	Hc
0.0	10.19	1.92	0.012
0.2	18.90	3.23	0.005
0.4	2.49	0.002	0.009

3.5 Biology effect of $Co_{1-x}Ni_xFe_2O_4$ferrite in bacteria :

Inhibition zone of E.coli bacteria

In figures (6)-(8) showed inhabitation zone of bacteria E.coli was the inhabitation zone about (15,15.5,16,16.5,16.5,16.9) for Co-Ni ferrite samples

Effect of Co-Ni ferrite in E.coli bacteria (Ni=0),it can explain alternating magnetic field that applied in E.coli bacteria lead to rise in temperatures between 40°C and 45°C are generally being referred to as hyperthermia. temperatures up to 42oC can render kill cells more susceptible to the effect of irradiation and cause a certain degree of apoptosis, whereas temperatures >45°C attributed with research. In figures (9) showed inhabitation zone of bacteria E.coli.

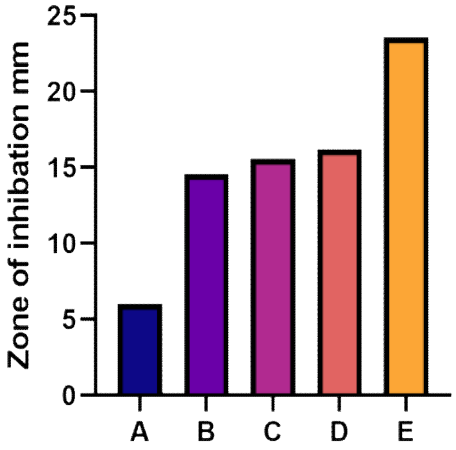

Figure (6) Inhibition zone of E.coli bacteria via Co-Niferrite enhancement (sample 1)

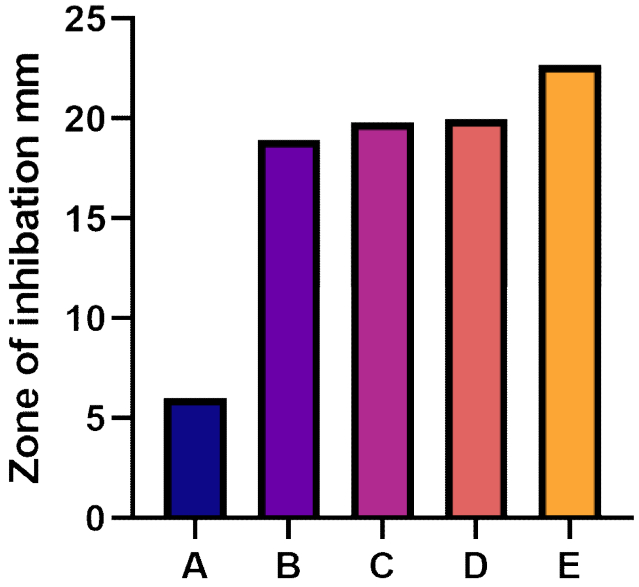

Figure (7) Inhibition zone of E.coli bacteria via Co-Niferrite enhancement (sample 2)

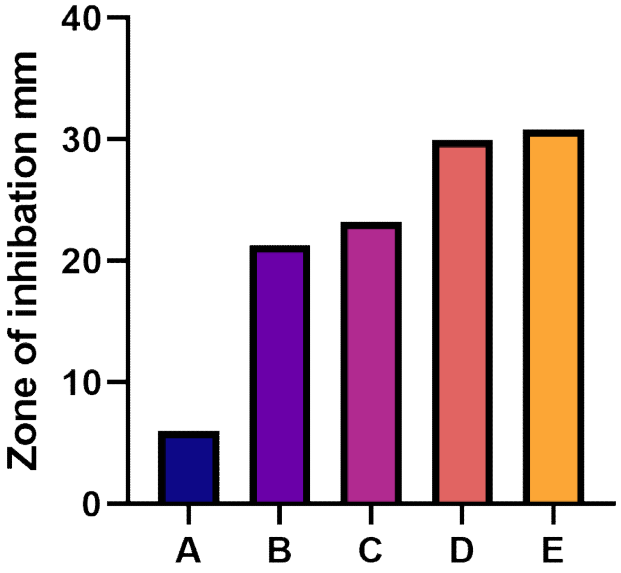

Figure (8) Inhibition zone of E.coli bacteria via Co-Niferrite enhancement (sample 3)

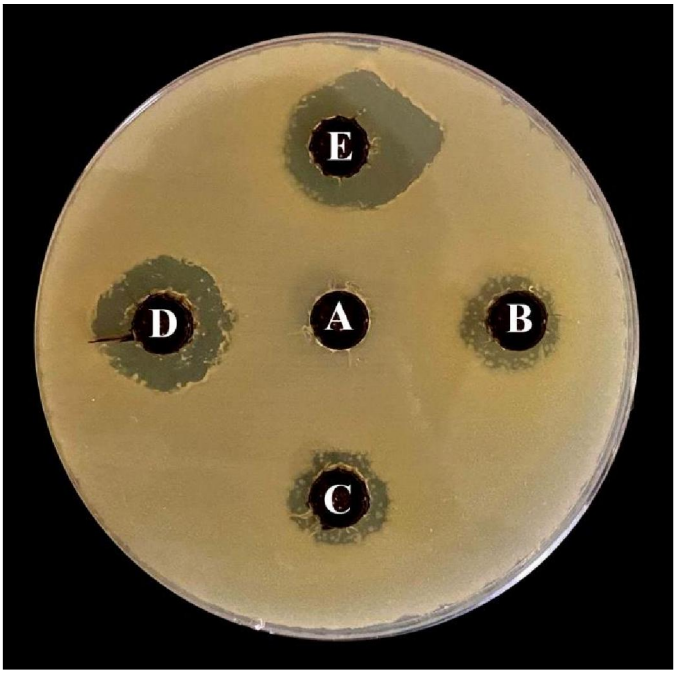

Figure (9): Inhibition zone of E.coli bacteria via Co-Ni ferrite

Table (4): Inhibition zone results of Co-Ni-Fe_2O_4ferriteby pulsed laser deposition(PLD) techniques, againts one type bacteria at 30 (mg/mL) concentrations.

SAMPLES	A	B	C	D	E
1	6	14.573	15.549	16.19	23.581
2	6	18.936	19.824	19.995	22.704
3	6	21.323	23.223	29.994	30.855

are responsible. To test the antibacterial efficacy of Co-Ni-Fe_2O_4 ferrite, researchers used growth inhibition zones to prevent the development of E. coli and Staphylococcus aureus, both gram-negative bacteria. Co-precipitated Co-Ni-Fe_2O_4 NCs had growth inhibition zones of 33 and 28.565 mm, respectively, when grown using this method. Using the pulsed laser deposition (PLD) approach, the Co-Ni-Fe_2O_4 NCs had narrower zones (31 mm and 20 mm, respectively). Using these NCs to treat infections caused by these bacteria is a possibility.

4. Conclusions

Cobalt-Nickel ferrite nanopowders with chemical formula of $Co_{1-x}Ni_xFe_2O_4$ (where, x= 0.0, 0.2, 0.4) were synthesized using plsd laser deposition method .The cubic spinel phase is seen in the ferrite samples' XRD patterns. As established by X-ray diffraction, the size of a single cubic spinel structure ranging from 9 to 15 nm is the typical crystalline size of ferrite nanoparticles. The nanocrystal lines in the produced products are confirmed by FESEM pictures. Infrared spectroscopy of the ferrite powders reveals two distinct bands in the 500-600 cm^{-1} and 385-450 cm^{-1} wavelength range, It is possible that the tetrahedral and octahedral complexes

[11] Dzmitry Kotsikaua, Vladimir Pankov, Elena Petrova, Valentin Natarov, Dmitry Filimonov and Konstantin Pokholok, Structural, magnetic and hyperfine characterization of ZnxFe3–xO4 nanoparticles prepared by sol-gel approach via inorganic precursors , Journal of Physics and Chemistry of Solids, vol.114, pp.64-70, (2018).

[12]G.Vaidyanathan, S.Sendhilnathan, and R,Arulmurugan," Structural and magnetic properties of $Co_{1-x}Zn_xFe_2O_4$ nanoparticles by co-precipitation method" Journal of Magnetism and Magnetic Materials, 313(2), 293-299,2007.

References

[1] G. man “Recent Advances in Ferrite Materials Technology”, in Mdern Ferrite Technology, Van Nostr and Reinhold, New York, (1990).

[2] P.K. Roy,” Magnetism and Magnetic Materials “ J.Bera , 298(1), p. 38-42(2006).

[3] J. Smit, H.P.J. Wijn, Ferrites, Jhon Wiley and Sons, NewYork, (1959).

[4] T. Gupta, "Handbook of Thick- and Thin-film HybridMicroelectronics," Hoboken, N.J.: Wiley-Interscience, 2003

[5]R. Eason, "Pulsed Laser Deposition of Thin Films: Applications-ledGrowth ofFunctional Materials,” Hoboken, NJ: Wiley-Interscience, 2007.

[6] S. Singh, N.K. Ralhan, R.K. Kotnal, K.C. Verma, Nanosize dependent electircal and magnetic properties of NiFe2O4 ferrites. Indian J. Pure Appl. Phys. 50, 739–743 (2012)

[7] Nga H. N. Do, Thao P. Luu, Quoc B. Thai, Duyen K. Le, Ngoc Do Quyen Chau, Son T. Nguyen, Phung K. Le, Nhan Phan-Thien & Hai M. Duong (2019): Advanced fabrication and application of pineapple aerogels from agricultural waste, Materials Technology, DOI: 10.1080/10667857.2019.1688537.

[8] Dalia M. S.A. Salem et al.,Biogenic synthesis and antimicrobial potency of iron oxide (Fe3O4) nanoparticles using algae harvested from the Mediterranean Sea, Egypt, The Egyptian Journal of Aquatic ResearchVolume 45, Issue 3, September 2019, Pages 197-204. https://doi.org/10.1016/j.ejar.2019.07.002

[9] Abid, M. A., & Kadhim, D. A. (2021). Synthesis of iron oxide nanoparticles by mixing chilli with rust iron extract to examine antibacterial activity. Materials Technology, 1-10.

[10] Ashour, A.H., El-Batal, A.I., AbdeMaksoud, M.I.A., El-Sayyad, G.S., Labib, S., Abdeltwab, E., and El-Okr, M.M. Antimicrobial activity of metal-substituted cobalt ferrite nanoparticles synthesized by sol-gel technique. Particuology, Vol. 40, Pp. 141–151, 2018